

Structures and Dynamics of Lanthanide(III) Complexes of Sugar-Based DTPA-bis(amides) in Aqueous Solution: A Multinuclear NMR Study

Hendrik Lammers,[†] Frédéric Maton,[‡] Dirk Pubanz,[§] Martijn W. van Laren,[†]
Herman van Bekkum,[†] André E. Merbach,^{*,§} Robert N. Muller,^{*,‡} and Joop A. Peters^{*,†}

Laboratory of Organic Chemistry and Catalysis, Delft University of Technology, Julianalaan 136, 2628 BL Delft, The Netherlands, NMR Laboratory, Department of Organic Chemistry, University of Mons-Hainaut, B-7000 Mons, Belgium, and Institute of Inorganic and Analytical Chemistry, University of Lausanne-BCH, CH-1015 Lausanne, Switzerland

Received November 14, 1996[⊗]

The structure and dynamics of the lanthanide(III) complexes of DTPA-BGLUCA³⁻ (DTPA-bis(glucamide)), DTPA-BENGALAA³⁻ (DTPA-bis(ethylenegalactamine-amide)), DTPA-BEA³⁻ (DTPA-bis(ethanolamide)), and DTPA-BPDA³⁻ (DTPA-bis(propanediolamide)) in water have been investigated. These complexes are of relevance as potential MRI contrast agents. ¹³C relaxation times of the Nd(III) complexes show octadentate binding of the organic ligand via the three amines, the three carboxylates, and the two amide oxygens. ¹⁷O NMR measurements indicate that the coordination sphere is completed by one water ligand. Eight diastereomeric pairs of isomers are observed for the DTPA-bis(sugaramides). Data sets obtained from variable-temperature and -pressure ¹⁷O NMR at 9.4 T and variable-temperature ¹H nuclear magnetic relaxation dispersion (NMRD) on the Gd(III) complexes were fitted simultaneously to give insight into the parameters governing the water ¹H relaxivity. The water exchange rates, k_{ex} ²⁹⁸, on [Gd(DTPA-BPDA)(H₂O)], [Gd(DTPA-BGLUCA)(H₂O)] and [Gd(DTPA-BENGALAA)(H₂O)] are 3.6 ± 0.3 , 3.8 ± 0.2 , and $2.2 \pm 0.1 \times 10^5 \text{ s}^{-1}$, and the activation volumes are +6.7, +6.8, and +5.6 cm³ mol⁻¹ ($\pm 0.2 \text{ cm}^3 \text{ mol}^{-1}$), respectively, indicating a strongly dissociatively activated mechanism. The sugar moieties have no significant influence on the coordination of the Gd(III) ion and on the parameters governing the relaxivity, apart from the expected increase in the rotational correlation time. The relaxivity under the usual MRI conditions is limited by the water exchange rate and the electronic relaxation. The data obtained are used to explain the relaxivity of conjugates of polysaccharides and Gd(DTPA).

Introduction

The rapid development of biomedical magnetic resonance imaging (MRI) as a clinical modality provoked a prodigious growth in interest in lanthanide(III) complexes for application as contrast agents.^{1–5} These agents enhance proton relaxation rates ($1/T_1$ and $1/T_2$) of water, and since these parameters determine the intensity of the NMR signal, the contrast of images may be improved. All current commercially available MRI contrast reagents for clinical use are polyamino polycarboxylate complexes of Gd(III), such as [Gd(DTPA)(H₂O)]²⁻ (DTPA = diethylenetriamine-*N,N,N',N',N''*-pentaacetate), Gd(DTPA-BMA)(H₂O) (DTPA-BMA = DTPA-bis(methylamide), [Gd(DOTA)(H₂O)]⁻ (DOTA = 1,4,7,10-tetraazacyclododecane-1,4,7,10-tetraacetate), and Gd(HP-DO3A)(H₂O) (HP-DO3A = 10-(2-hydroxypropyl)-1,4,7,10-tetraazacyclododecane-1,4,7-triacetate). The Gd(III) ion is especially suitable because of its high electron spin ($S = 7/2$) and relatively slow electronic relaxation. Therefore high relaxivity is produced by the

fluctuating dipole–dipole interaction between the electron spin of the paramagnetic center and the proton nuclear spin.

Around a paramagnetic ion, the bulk water proton relaxation rates are enhanced due to long-range interactions (“outer-sphere” relaxation) and short-range interactions (“inner-sphere” relaxation). According to the standard Solomon–Bloembergen–Morgan model, the latter process is governed by four correlation times: the time for rotation of the complex, τ_R ; the residence time of a water proton in the inner coordination sphere, τ_m ; the electronic longitudinal and transverse relaxation rates ($1/T_{1e}$ and $1/T_{2e}$) of the metal center.^{3–6} The outer-sphere relaxivity is determined by the relative diffusional motion of outer-sphere water molecules and the complex and by $1/T_{1e}$ and $1/T_{2e}$.⁶ The “inner-sphere” and “outer-sphere” contributions to the proton relaxivity in these complexes are similar in magnitude.

The evolution of the MRI technique has given rise to an increasing demand for contrast agents that are more effective and specific than the ones currently commercially available. Theory predicts that it should be possible to make contrast agents with a relaxivity that is 50 times higher than that of the contrast agents presently in use. The rational design of improved contrast agents requires insight into the relation between structure and proton relaxation enhancement.^{3–7}

An option to achieve higher relaxivities is to couple the Gd chelates covalently to high molecular weight compounds, such as polysaccharides, in order to slow down the rotation.⁵ These

[†] Delft University of Technology.

[‡] University of Mons-Hainaut.

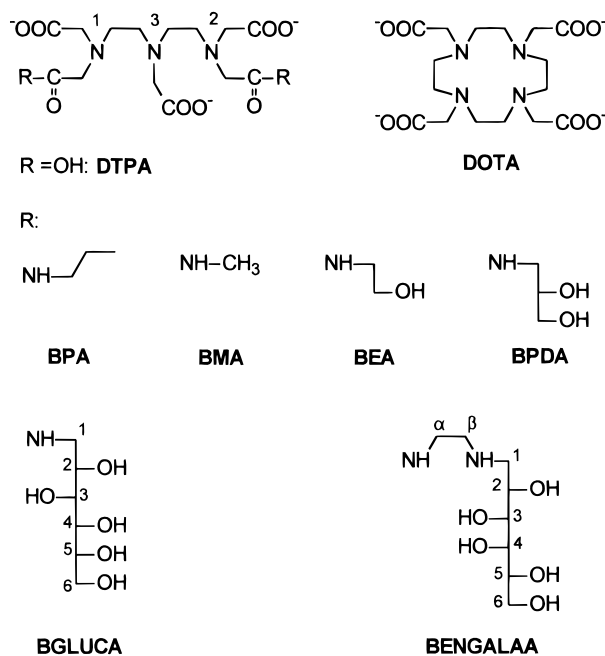
[§] University of Lausanne.

[⊗] Abstract published in *Advance ACS Abstracts*, May 1, 1997.

- (1) Rocklage, S. M.; Watson, A. D.; Carvlin, M. J. In *Magnetic Resonance Imaging*, 2nd ed.; Stark, D. D., Bradley, W. G., Eds.; Mosby Year Book: St Louis, MO, 1992; Chapter 14.
- (2) Choppin, G. R.; Schaab, K. M. *Inorg. Chim. Acta* **1996**, 252, 299.
- (3) Lauffer, R. B. *Chem. Rev.* **1987**, 87, 901.
- (4) Tweedle, M. F. In *Lanthanide Probes in Life, Chemical and Earth Sciences*; Bünzli, J.-C. G., Choppin, G. R., Eds.; Elsevier: Amsterdam, 1989; Chapter 5.
- (5) Peters, J. A.; Huskens, J.; Raber, D. J. *Prog. Nucl. Magn. Reson. Spectrosc.* **1996**, 28, 283.

(6) Koenig, S. H.; Brown, R. D., III. *Prog. Nucl. Magn. Reson. Spectrosc.* **1990**, 22, 487 and references therein.

(7) Geraldès, C. F. G. C.; Sherry, A. D.; Cacheris, W. P.; Kuan, K. T.; Brown, R. D., III; Koenig, S. H.; Spiller, M. *Magn. Reson. Med.* **1988**, 8, 191.

Chart 1. Structures of the Various Ligands Discussed

types of high molecular weight contrast agent are being investigated for their potential use as blood pool agents. Introduction of sugar compounds in the proximity of the Gd(III) ion may influence the various parameters governing the relaxivity. Here we report on a multinuclear NMR study of the structure and dynamics of the Ln(III) complexes of DTPA-BGLUCA³⁻ and DTPA-BENGALAA³⁻ and of the model compounds DTPA-BEA³⁻ and DTPA-BPDA³⁻ in aqueous solution (see Chart 1 for the structures) which may serve as model compounds for DTPA-linked polysaccharides. The various Ln(III) complexes of a particular ligand are usually nearly isostructural. One can therefore profit from the different NMR properties of the various Ln(III) ions in the analysis of the solution structures of these complexes.⁵ A comprehensive study of the parameters governing the relaxivity has been undertaken using variable-temperature and -pressure ¹⁷O measurements and NMRD profiles recorded at various temperatures.

Experimental Section

Materials. All chemicals were purchased from Aldrich Chemical Co. unless otherwise specified and were used without any further purification. The lanthanide content of the hydrated lanthanide chlorides was determined by chelatometric titration with EDTA and xylenol orange as the indicator.

Synthesis of Ligands. General Procedure. Compounds DTPA-BGLUCA³⁻ and DTPA-BENGALAA³⁻ were prepared analogously to a procedure described by Konings *et al.*⁸ DTPA-bis(anhydride) (0.02 mol) was added in small portions to a stirred solution of 0.1 mol of the appropriate amine,^{9,10} dissolved in 25 mL distilled water. An excess of amine was used to avoid the formation of monosubstituted DTPA derivatives. After 2 h the solvent was evaporated and the resulting mixture was separated on a Dowex-H⁺ (25 × 4 cm) column by applying a gradient from 0 to 2.0 M aqueous HCl. The fractions containing the product were collected and, after adjustment of the pH to 7, were desalted by membrane filtration (UTC 60, Toray Industries, Inc., Tokyo, Japan, 20 bar pressure) and freeze-dried.

***N,N'*-Bis[*N*-(*D*-gluco-2,3,4,5,6-pentahydroxyhexyl)carbamoylmethyl]diethylenetriamine-*N,N',N''*-triacetic Acid (DTPA-**

BGLUCA). A white solid was obtained; yield = 3.5 g (45%). ¹H NMR (400 MHz, D₂O, pH 1.44): δ 4.23 (s, 4H, N²CH₂CO), 4.22 (s, 4H, N²CH₂CO), 3.88 (m, 2H, H-2, *J*_{1,2} = 4.0, *J*_{1',2} = 8.0, *J*_{2,3} = 5.5 Hz), 3.78 (dd, 2H, H-6, *J*_{5,6} = 3.0, *J*_{6,6'} = -11.5 Hz), 3.75-3.71 (m, 4H, H-3 and H-5), 3.65 (s, 2H, N¹CH₂COOH), 3.64 (m, 2H, H-4, *J*_{3,4} = 2.3, *J*_{4,5} = 8.0 Hz), 3.61 (dd, 2H, H-6', *J*_{5,6'} = 6.0 Hz), 3.56 (t, 2H, N²CH₂CH₂N¹, *J*_{H,H} = 6.3 Hz), 3.49 (dd, 2H, H-1, *J*_{1,1'} = -14.0 Hz), 3.34 (dd, 2H, H-1'), 3.18 (t, 2H, N²CH₂CH₂N¹). ¹³C NMR (50.3 MHz, D₂O, pH 2.56): δ 43.70 (C-1), 51.10 (N³CH₂CH₂N¹), 54.92 (N³CH₂-CH₂N¹), 55.32 (N³CH₂COO), 56.93, 57.89 (N¹CH₂COO, N¹CH₂CON), 64.31 (C-6), 71.80 (C-2), 72.42, 72.55, 72.76 (C-3, C-4, C-5), 167.54 (N¹CH₂CON), 170.32 (N³CH₂COO), 175.08 (N¹CH₂COOH). MS (*m/e*): 720 (MH⁺). Anal. Calcd (found) for C₂₆H₄₉N₅O₁₈: C, 43.39 (43.17); H, 6.82 (6.79); N, 9.74 (9.68); O, 40.06 (40.0).

***N,N''*-Bis[*N*-(3-aza-*D*-galacto-5,6,7,8,9-pentahydroxynonyl)carbamoylmethyl]diethylenetriamine-*N,N',N''*-triacetic Acid (DTPA-BENGALAA).** A slightly yellow hygroscopic solid was obtained; yield = 6.0 g (32%). ¹³C NMR (50.3 MHz, D₂O, pH 9.12): δ 38.70 (C-1), 48.87 (C-β), 52.57 (C-α), 54.45, 57.03 (N³CH₂COO), 60.41, 60.48 (N¹CH₂COO, N¹CH₂CON) 64.80 (C-6), 68.58 (C-2), 70.90, 71.62, 72.10 (C-3, C-4, C-5), 174.28 (N¹CH₂CON), 175.91 (N³CH₂COO), 180.60 (N¹CH₂COO). MS (*m/e*): 806 (MH⁺).

Deuteration of Derivatives of DTPA. Deuteration of the acetate functions of the DTPA derivatives was performed as described by Wheeler and Legg.¹¹ The ligand (0.4 g) was dissolved in 40 mL of D₂O, and the pD was adjusted to 10.6 by addition of K₂CO₃. The mixture was refluxed under stirring for 24 h. The pD was then adjusted to 2 by addition of aqueous HCl. The volume was reduced to 10 mL by evaporation of solvent, and the solid KCl was filtered off. Addition of acetone induced precipitation of the deuterated ligand, which was filtered off.

NMR Measurements. The La(III), Nd(III), and Gd(III) complexes of the ligands were prepared by mixing aqueous solutions of equimolar amounts of hydrated LnCl₃ and ligand. The absence of free Ln(III) was verified using a xylenol orange indicator.¹² After adjustment of the pH to approximately 7, NaCl was removed by membrane filtration. The solutions were freeze-dried, and the complexes were obtained as the trihydrates. Samples of the Ln(III) complexes for the NMR measurements were prepared by dissolution of solid Ln(III) complex or by dissolving equimolar amounts of ligand and hydrated LnCl₃ in weighted amounts of D₂O. The pH of the solutions was measured at room temperature with a calibrated micro-combination probe purchased from Aldrich Chemical Co. The pH values given are direct meter readings. For the variable-temperature and -pressure ¹⁷O NMR measurements the samples were dissolved in 10% ¹⁷O-enriched water and the pH was adjusted with weighted amounts of 0.01 m (mol/kg of water) HClO₄.

The complete spectral assignment of DTPA-BGLUCA³⁻ was carried out by means of ¹H homonuclear correlation spectroscopy (COSY) and ¹H-¹³C chemical shift correlation spectroscopy (HETCOR).

The ¹⁷O and ¹³C NMR spectra were recorded with a Nicolet NT-200 WB or a Varian VXR-400 S spectrometer. For ¹³C NMR *t*-BuOH (methyl signal at 31.2 ppm) was used as the internal standard. The ¹⁷O chemical shifts were recorded with respect to D₂O as external standard (substitution method); the chemical shifts were determined by fitting the observed signal with a Lorentzian line function. Downfield shifts are denoted as positive.

The compositions of the samples used in the variable-temperature and -pressure ¹⁷O NMR measurements are given in Table 1. Variable-temperature ¹⁷O NMR measurements were performed at a magnetic field of 9.4 T using either a Varian VXR-400 S spectrometer equipped with a cold junction temperature control unit (Thermo Electric) or a Bruker AM-400 spectrometer equipped with Bruker VT-1000 temperature control unit. The temperature was stabilized within 0.1 °C of the desired value and was measured by a substitution technique.¹³ The samples were sealed in glass spheres, fitting into 10 mm NMR tubes,

(8) Konings, M. S.; Dow, W. C.; Love, D. B.; Raymond, K. N.; Quay, S. C.; Rocklage, S. M. *Inorg. Chem.* **1990**, *29*, 1488.

(9) Kelkenberg, H. *Tens. Surf. Det.* **1988**, *25*, 8.

(10) Lammers, H.; Peters, J. A.; van Bekkum, H. *Tetrahedron* **1994**, *50*, 8103.

(11) Wheeler, W. D.; Legg, J. I. *Inorg. Chem.* **1985**, *24*, 1292.

(12) Brumisholz, G.; Randin, M. *Helv. Chim. Acta* **1959**, *42*, 1927.

(13) Amman, C.; Meyer, P.; Merbach A. E. *J. Magn. Reson.* **1982**, *46*, 319.

Table 1. Compositions of the Aqueous Solutions Used in the Variable-Temperature ^{17}O NMR and Variable-Pressure ^{17}O NMR Spectrometry Measurements^a

no.	solution	[Ln(III)] (mol kg ⁻¹)	10 ³ P _m	pH
1	acidified water			4.35
2	[Gd(DTPA-BPDA)(H ₂ O)]	0.155	2.79	4.38
3	[Gd(DTPA-BGLUCA)(H ₂ O)]	0.191	3.44	4.38
4	[Gd(DTPA-BENGALAA)(H ₂ O)]	0.204	3.68	4.35

^a All solutions were in ^{17}O -enriched water (2–10% enrichment).

in order to eliminate bulk susceptibility effects on the chemical shift.¹⁴ Longitudinal relaxation rates, $1/T_1$, were obtained by the inversion-recovery method,¹⁵ and transverse relaxation rates, $1/T_2$, were measured by the Carr–Purcell–Meiboom–Gill spin-echo technique¹⁶ or, for line widths larger than 1 kHz, directly from the line widths. At each temperature, the spectral parameters were measured for both a sample with the Gd(III) complex and a sample of acidified water (pH 4.35) under exactly the same conditions. No frequency lock was applied. Variable-pressure NMR measurements were carried out up to 200 MPa on a Bruker AM-400 spectrometer equipped with a home-built probe head.¹⁷ The temperature was controlled by circulating fluid from a temperature bath and was measured using a built-in Pt resistor. The transverse relaxation rates were measured in the same way as had been done for the variable-temperature work.

Deuterium longitudinal relaxation rates were measured at 4.7 T on a Bruker MSL 200-15 spectrometer and a broadband probe using 2 mL of sample contained in 10 mm o.d. tubes. The solvent (water) was deuterium depleted. No frequency lock was used. The temperature was regulated by air or nitrogen flow controlled by a BVT 1000 or BVT 2000 Bruker unit. The 90° and 180° pulse lengths were equal to 9 and 18 μs, respectively. The concentration of the deuterated compound was lower or equal to 50 mM. T_1 measurements were performed with the inversion recovery or fast inversion recovery Fourier transform technique and a three-parameter fitting of the peak heights. The number of averaged transients was 100.

NMRD Measurements. The $1/T_1$ nuclear magnetic relaxation dispersion (NMRD) profiles of the solvent protons at several temperatures were obtained on an IBM Research Relaxometer, using the field cycling method and covering a continuum of magnetic fields from 2.5×10^{-4} to 1.2 T (corresponding to a proton Larmor frequency range 0.01–50 MHz). The absolute uncertainty in the $1/T_1$ for the NMRD measurements was ±3%. The spin–lattice proton relaxation rates at 20 MHz were also measured on a spin analyzer Multispec Bruker PC-20. The proton relaxation rates at 4.7 and at 9.4 T (proton Larmor frequencies of 200 and 400 MHz, respectively) were determined by the inversion recovery Fourier transform technique on a Bruker MSL-200 and a Varian VXR-400 S spectrometer.

Fast atom bombardment (FAB) spectra were obtained with a VG 70-250 SE mass spectrometer. Elemental analyses were performed by Mikroanalytisches Labor Pascher, Remagen, Germany.

Results and Discussion

Ln(III)-Induced Water ^{17}O Shifts. Upon addition of Dy(III) to a 0.08 M solution of one of the ligands under study in D₂O at pD 7, the water ^{17}O shift decreased linearly as the molar ratio Dy(III)/L (ρ_L) increased. At $\rho_L = 1.0$, a large increase occurred in the magnitude of the (negative) induced shift. The exchange of water between the Dy(III) complex and the bulk is fast on the ^{17}O NMR time scale under the conditions applied (4.7 T, 75 °C). From the break in the curves it can be concluded that all ligands form 1:1 complexes at $\rho_L \leq 1$. For DTPA-BGLUCA³⁻ (Figure 1), the slope of the line $\rho_L > 1$ was 8.1 times larger than that of the line $\rho_L < 1$ and identical to the

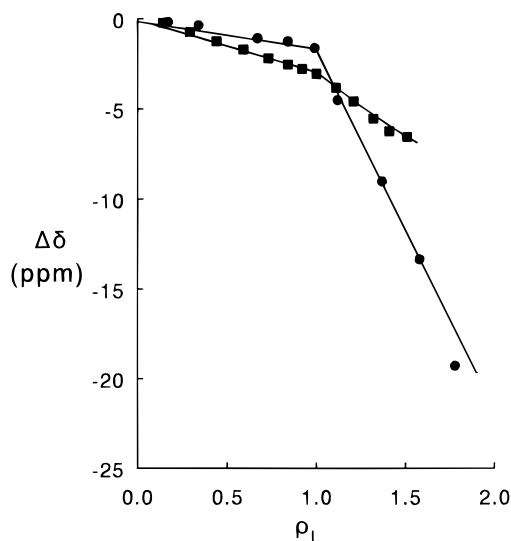


Figure 1. Plots of the Dy(III)-induced water ^{17}O shift versus the molar ratio Dy(III)/organic ligand (ρ_L) for 0.08 M solutions of DTPA-BGLUCA (●) and DTPA-BENGALAA³⁻ (■) in D₂O at 75 °C and pH 7.

slope of the line obtained when the titration with Dy(III) was performed in the absence of DTPA-BGLUCA³⁻. Similar plots were obtained with DTPA-BEA³⁻ and DTPA-BPDA³⁻, but the plot for DTPA-BENGALAA³⁻ had a different shape (Figure 1). There the slope at $\rho_L > 1$ was only about one-third of the slope of the line obtained in the absence of an organic ligand. At $\rho_L > 1.4$ a precipitate formed.

Previously, the Dy(III)-induced ^{17}O water shifts were shown to be independent of the other ligands chelated to the Dy(III) ion and to be predominantly of contact origin ($\geq 85\%$).¹⁸ Consequently, the slope of a plot of the Dy(III)-induced shift versus the molar ratio Dy(III)/water (ρ_w) is proportional to the hydration number of the Dy(III) complex. If it is assumed that the Dy(III) aquo ion contains 8 water ligands,¹⁹ then it can be concluded that all complexes under study contain one water molecule in the first coordination sphere of the Dy(III) ion at $\rho_L \leq 1$. Commonly, the Ln(III) ion in complexes of this type has a coordination number of 9. This suggests that the organic ligand is coordinated in an octadentate fashion. Most likely the donor sites are the same as for the previously investigated DTPA-BPA³⁻ ligand: the three nitrogens of the diethylenetriamine group; three carboxylate oxygens; the two amide oxygens.²⁰

The deviation of the Dy–DTPA-BENGALAA³⁻ system at $\rho_L > 1$ can be explained by the formation of a di- or oligonuclear species at these concentrations. At lower pH values (pH 4), the secondary amine functions in the sugar side chains are fully protonated and then the curves of Dy(III)-induced ^{17}O water shifts versus ρ are similar to those of the other ligands at all ρ values. Further studies on the structure of the Ln(DTPA-BENGALAA) complexes are in progress.

In order to obtain the number of inner-sphere water molecules in the other Ln(III) complexes, a more extended treatment of the Ln(III)-induced water ^{17}O shifts is required. The induced shifts (Δ) comprise diamagnetic (Δ_d), contact (Δ_c), and pseudo-contact shifts (Δ_p). The value of Δ_d can be estimated from an interpolation of the induced shifts for La(III) and Lu(III). The

(14) Hugi, A. D.; Helm, L.; Merbach, A. E. *Helv. Chim. Acta* **1985**, *68*, 508.

(15) Vold, R. V.; Waugh, J. S.; Klein, M. P.; Phelps, D. E. *J. Chem. Phys.* **1968**, *48*, 3831.

(16) Meiboom, S.; Gill, D. *Rev. Sci. Instrum.* **1958**, *29*, 688.

(17) Frey, U.; Helm, L.; Merbach, A. E. *High Pressure Res.* **1990**, *2*, 237.

(18) Alpoim, M. C.; Urbano, A. M.; Galdes, C. F. G.; Peters, J. A. *J. Chem. Soc., Dalton Trans.* **1992**, 463 and references therein.

(19) Kowall, Th.; Foglia, F.; Helm, L.; Merbach, A. E. *J. Am. Chem. Soc.* **1995**, *117*, 3790.

(20) Galdes, C. F. G.; Urbano, A. M.; Hoefnagel, M. A.; Peters, J. A. *Inorg. Chem.* **1993**, *32*, 2426.

Table 2. Lanthanide-Induced Water ^{17}O Shifts (ppm) for 0.1 M Ln(DTPA-BEA), Ln(DTPA-BPDA), and Ln(DTPA-BGLUCA) Complexes in D_2O at pD 7 and 75 °C

Ln(III)	δ (ppm) ^a		
	DTPA-BEA ³⁻	DTPA-BPDA ³⁻	DTPA-BGLUCA ³⁻
La	964	790	431
Pr	935	1171	938
Nd	1174	1074	681
Eu	-80	-175	-362
Tb	-1985	-2305	-2110
Dy	-1672	-2085	-1938
Ho	-1107	-998	-1410
Er	-88	24	-44
Tm	600	580	639
Yb	772	670	716
Lu	729	921	363
<i>qF</i>	-68	-78	-74
<i>qG</i>	11.0	7.2	8.7

^a The shifts were obtained using plots analogous to that given in Figure 1. The values are extrapolated to a molar ratio of Ln(III)/water (ρ_w) = 1. The relative errors are 5%.

contact contribution results from a through-bond transmission of unpaired spin density, whereas the pseudocontact shift arises from a through-space dipolar interaction between the magnetic moments of the unpaired electrons of the Ln(III) ion and the ^{17}O nucleus. Both Δ_c and Δ_p can be written as the product of a term that is characteristic of the Ln(III) ion but independent of the complex structure ($\langle S_z \rangle$ and C^D , respectively) and a second term that is characteristic of the complex but that is independent of the Ln(III) ion (F and G , respectively):^{21,22}

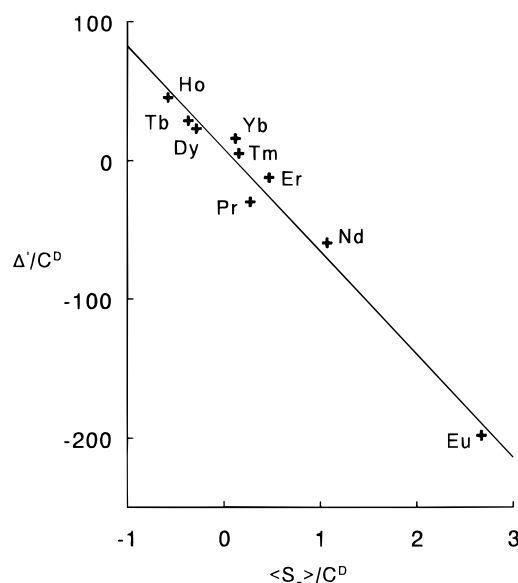
$$\Delta' = \Delta - \Delta_d = \Delta_c + \Delta_p = \langle S_z \rangle F + C^D G \quad (1)$$

Values for $\langle S_z \rangle$ and C^D are tabulated in the literature.²¹⁻²⁵ When the various Ln(III) complexes are isostructural, eq 1 can be rearranged in a linear form:²⁶

$$\Delta'/C^D = \langle S_z \rangle F/C^D + G \quad (2)$$

Thus, when a series of Ln(III) complexes yields a linear plot of Δ'/C^D versus $\langle S_z \rangle/C^D$, this indicates that they are isostructural.^{26,27}

The water ^{17}O shifts for the various Ln complexes of DTPA-BEA³⁻, DTPA-BPDA³⁻, and DTPA-BGLUCA³⁻ at 75 °C were extrapolated to $\rho_w = 1$ (Table 2). The values obtained correspond to $q\Delta$, where q is the number of the bound waters in the concerning complex. Plotting of the shifts according to eq 2 gave straight lines for the three ligands. In Figure 2 this is illustrated for DTPA-BGLUCA³⁻. These results show that there is no change in the hydration number of these complexes along the Ln series. The values of qF and qG determined by means of a multiple regression method²⁸ are given in Table 2. Previous investigations have shown that the values of F for Ln(III)-bound oxygens fall in a narrow range of -70 ± 11 at 73 °C.²⁹⁻³¹ It can be concluded that the hydration number does

**Figure 2.** Plot of Δ'/C^D versus $\langle S_z \rangle/C^D$ for the ^{17}O signal in the Ln-DTPA-BGLUCA system at 75 °C.

not change across the lanthanide series. Therefore, the stoichiometry of the chelates mentioned above in solution ($\rho_L \leq 1$) is [Ln(DTPA-bis(amide))(H₂O)].

^{13}C NMR Spectra. Upon octadentate binding of the DTPA-bis(amide) ligands to Ln(III) ions in a mode as suggested by the results of the ^{17}O measurements, inversion of the three nitrogen atoms of the diethylenetriamine backbone is precluded. Therefore, these atoms are chiral and the ligand can occur in eight enantiomeric forms. If it is assumed that the coordination polyhedron of the nine-coordinated Ln(III) ion in these complexes can be described by a tricapped trigonal prism, this gives rise to the eight complex geometries depicted in Figure 3. Similar isomers are possible for a monocapped square antiprism. Previously, it has been shown that all eight isomers occur in aqueous solutions of the Ln(III) complexes of DTPA-BPA³⁻.²⁰ Two dynamic processes play an important role: (i) racemization of the central nitrogen atom via the interconversions of **1-4** and **1'-4'**, which are associated with the interconversions of the two gauche conformations of the ethylenediamine bridges ("wagging"); (ii) racemization at the terminal nitrogens via the interconversions **1** \rightleftharpoons **2** \rightleftharpoons **3** \rightleftharpoons **4** and **1'** \rightleftharpoons **2'** \rightleftharpoons **3'** \rightleftharpoons **4'**, which are relatively slow because they require decoordination of a nitrogen and its two neighboring oxygens (Figure 3).

The ^{13}C NMR spectra of the diamagnetic (La(III)) and paramagnetic (Nd(III)) complexes of the ligands DTPA-BEA³⁻, DTPA-BPDA³⁻, DTPA-BGLUCA³⁻, and DTPA-BENGALAA³⁻ displayed several resonances for each atom, which is consistent with the occurrence of various isomers in solution. In the static situation of compounds with a chiral side chain, each ligand nucleus would give rise to eight resonances. In addition to this, it should be noted that the two amide groups and the two terminal carboxylate groups in each isomer are chemically inequivalent. Thus, for the amide C- α atom, for example, 16 resonances are expected. When the "wagging" process is rapid on the NMR time scale, the number of signals is reduced to 8. Accordingly, the ^{13}C NMR spectrum of the Nd(DTPA-BGLUCA) complex in D_2O at 100.6 MHz and 80 °C shows eight signals for the amide C- α (δ 37-41, Figure 4). Upon decrease of the temperature to 0 °C, substantial line broadening

- (21) Golding, R. M.; Halton, M. P. *Aust. J. Chem.* **1972**, *25*, 2577.
 (22) Bleaney, B. *J. Magn. Reson.* **1972**, *8*, 91.
 (23) Bleaney, B.; Dobson, C. M.; Levine, B. A.; Martin, R. B.; Williams, R. J. P.; Xavier, A. V. *J. Chem. Soc., Chem. Commun.* **1972**, 791.
 (24) Golding, R. M.; Pyykkö, P. *Mol. Phys.* **1973**, *26*, 1389.
 (25) Pinkerton, A. A.; Rossier, M.; Spiliadis, S. *J. Magn. Reson.* **1985**, *64*, 420.
 (26) Reuben, J. *J. Magn. Reson.* **1982**, *50*, 233.
 (27) Peters, J. A. *J. Magn. Reson.* **1986**, *68*, 240.
 (28) Reilley, R. N.; Good, B. W.; Allendoerfer, R. D. *Anal. Chem.* **1976**, *48*, 1446.
 (29) Vijverberg, C. A. M.; Peters, J. A.; Kieboom, A. P. G.; van Bekkum, H. *Recl. Trav. Chim. Pays-Bas* **1980**, *99*, 403.

- (30) Peters, J. A.; Nieuwenhuizen, M. S.; Raber, D. J. *J. Magn. Reson.* **1985**, *65*, 417.
 (31) Nieuwenhuizen, M. S.; Peters, J. A.; Sinnema, A.; Kieboom, A. P. G.; van Bekkum, H. *J. Am. Chem. Soc.* **1985**, *107*, 12.

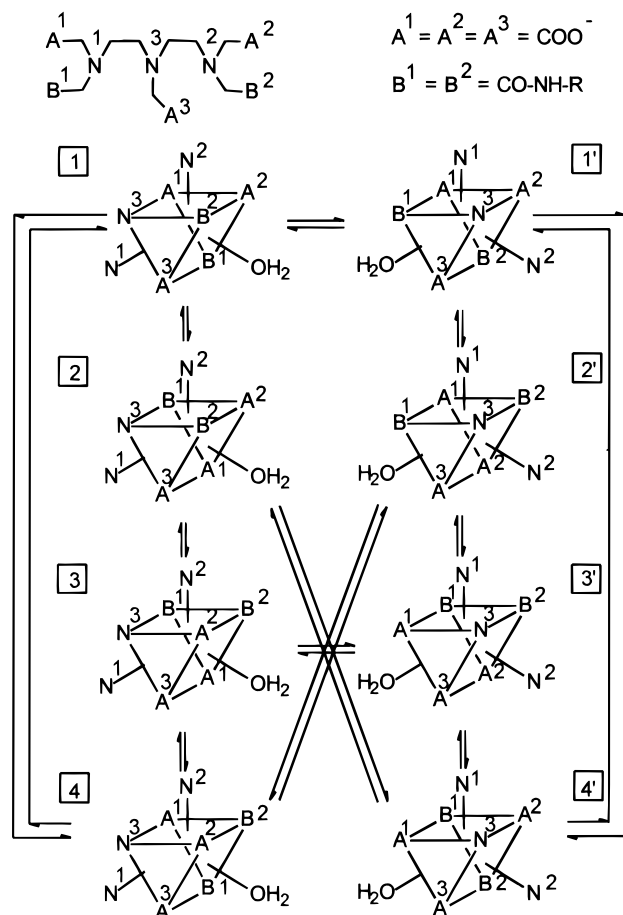


Figure 3. Coordination polyhedrons of the enantiomers of the Ln(DTPA-bis(amide)) complexes, assuming that the geometry is a tricapped trigonal prism. With nonchiral side chains no discrimination can be made between A^1 and A^2 , B^1 and B^2 , and N^1 and N^2 . These groups are labeled in order to be able to follow them during the rearrangements ($A^1 = A^2 = A^3 = \text{COO}^-$; $B^1 = B^2 = \text{CO-NH-sugar}$).

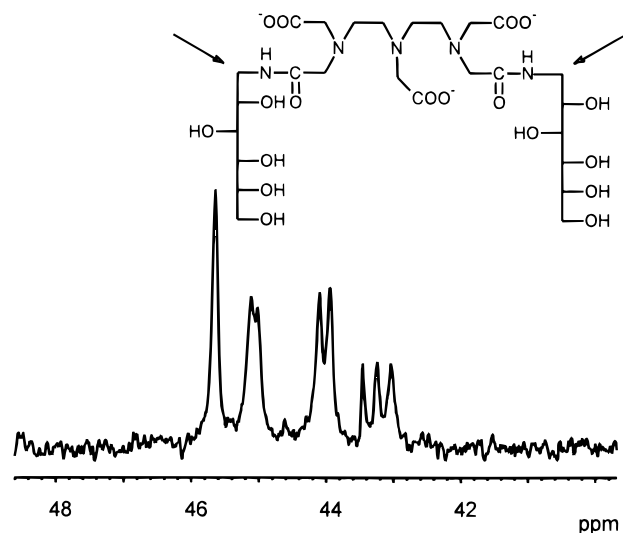


Figure 4. ^{13}C NMR spectrum (C- α region) of 0.1 M $[\text{Nd}(\text{DTPA-BLUCa})(\text{H}_2\text{O})]$ in D_2O at 80 °C and 100.6 MHz.

occurred. However, the slow-exchange region for the racemization around the central nitrogen atom could not be reached because further cooling, after addition of methanol, caused precipitation of the complex.

The ^{13}C spectrum of the Nd(DTPA-BEA) complex, in which the amide side chains are not chiral, shows fewer resonances than the Nd(DTPA-BGLUCA) complex. Here, the isomers 1'–

Table 3. Kinetic Data for the Racemization at N^1 and N^2 in La(DTPA-bis(amide)) Complexes at 283 K

ligand	ΔG^\ddagger (kJ mol $^{-1}$)	ΔH^\ddagger (kJ mol $^{-1}$)	ΔS^\ddagger (J mol $^{-1}$ K $^{-1}$)	k^{283} (s $^{-1}$)
DTPA-BGLUCA $^{3-}$ ^a	66	34	-116	2.7
DTPA-BENGALAA $^{3-}$ ^a	65	37	-100	5.2
DTPA-BPA $^{3-}$ ^{b,c}	71	47	-84	0.7

^a From coalescence temperatures of ^{13}C NMR signals (100.6 MHz).
^b From ^{13}C NMR line shapes (100.6 MHz). ^c Reference 20.

4' are the mirror images of 1–4 and thus not distinguishable with NMR. Consequently, only four resonances are observed for the amide C- α atom under conditions of rapid exchange on the NMR time scale among 1–4 and 1'–4'. This simplification is also observed in the ^{13}C NMR spectra of the Nd(III) complexes of DTPA-BPDA $^{3-}$ and DTPA-BENGALAA $^{3-}$, which both display only four signals in the C- α window at 80 °C and 100.6 MHz (Supporting Information). The chiral entity in DTPA-BENGALAA is probably too far away to be sensed by C- α , whereas the effects of chirality in the ^{13}C spectrum of DTPA-BPDA are possibly averaged-out by fast rotations in the PDA side chain.

The various isomers present in solution of each Nd(III) complex studied occur in unequal amounts as can be seen from the different signal intensities of, e.g., the amide C- α (Supporting Information). The region in the ^{13}C spectrum between 56 and 74 ppm (DTPA-backbone and sugar chain), in which the other signals appeared, was very complex due to severe overlapping. The methylene carbons of the diethylenetriamine group and the central glycine unit of the Ln(III) complexes (Ln = La, Nd) of the discussed chelates are at approximately the same chemical shifts as those of LnDTPA and LnDTPA-BPA complexes^{20,32} (Supporting Information). This confirms that there is both a similarity among the various Ln complexes discussed in this work and between these complexes and LnDTPA and LnDTPA-BPA.

In Table 3 the kinetic data for the racemization at N^1 , N^2 in LaDTPA-BGLUCA and LaDTPA-BENGALAA as determined by coalescence temperatures of the ^{13}C NMR signals at 100.6 MHz are presented. The activation parameters for this process are in good agreement with those obtained for LaDTPA-BPA indicating that the presence of the polyhydroxy chain does not alter significantly the dynamics of this particular intramolecular rearrangement.

Nd(III)-Induced Relaxation Rate Enhancements. Among the lighter Ln(III) ions (Ln = Ce \rightarrow Eu), Nd(III), having the longest electron relaxation times,^{33,34} was selected for the ^{13}C NMR longitudinal relaxation rate study on the coordination with the ligands discussed in this work. The Nd(III)-induced ^{13}C NMR relaxation enhancements have been measured for DTPA-BEA $^{3-}$, DTPA-BPDA $^{3-}$, DTPA-BGLUCA $^{3-}$, and DTPA-BENGALAA $^{3-}$ at 9.4 T and 80 °C. Under these conditions fast exchange on the NMR time scale occurs between several ligand nuclei due to the racemization at N^3 . In order to correct for diamagnetic contributions, the relaxation rates for the corresponding La(III) complex were subtracted from the measured values of the Nd(III) complex.

Since various isomers occur in solution, the relaxation rates obtained are weighted averages for these structures. If there are, for example, two species A and B, which are in fast exchange on the NMR time scale, the observed longitudinal

(32) Peters, J. A. *Inorg. Chem.* **1988**, *27*, 4686.

(33) Alsaadi, B. M.; Rossotti, F. J. C.; Williams, R. J. P. *J. Chem. Soc., Dalton Trans.* **1980**, 2151.

(34) Bertini, I.; Capozzi, F.; Luchinat, C.; Nicastro, G.; Xia, Z. *J. Phys. Chem.* **1993**, *97*, 6351.

Table 4. ^{13}C NMR Relaxation Data for 0.2 M Solutions of Ln(III) Complexes in D_2O at 80 °C and 100.6 MHz

nucleus	DTPA-BEA $^{3-}$	DTPA-BPDA $^{3-}$	DTPA-BGLUCA $^{3-}$	DTPA-BENGALAA $^{3-}$	
$1/T_1$ in Nd(III) Complex (s^{-1})					
CO	5.04–7.87	7.20–11.20	8.00–10.74	13.94–16.40	10.08–14.13 ^a
CH ₂ O	7.06–8.13	8.65–11.35	8.99–12.35	17.01–18.60	18.11 ^a
NCH ₂ CH ₂ O	7.19–7.37	10.63–11.10	11.15–11.49	17.49–19.88	20.33–25.93 ^a
C- α	1.47–1.53	2.55–2.61	3.95–4.58	6.71–6.90	8.88–10.40 ^a
$1/T_1$ in La(III) Complex (s^{-1})					
CO	0.16–0.23	0.33–0.42	0.35–0.40	0.82–0.91	0.65–1.06 ^a
CH ₂ O	2.08–2.16	4.14–4.55	4.48–4.69	6.17–6.65	9.33–10.95 ^a
NCH ₂ CH ₂ O	2.42–2.48	4.89–5.45	5.06–5.37	7.59–8.35	12.78–13.37 ^a
C- α	1.06	2.24–2.34	3.26	6.01	8.98
NOE Effects in La(III) Complex					
CH ₂ O	1.90	1.67	1.57	1.32	
NCH ₂ CH ₂ O	1.68	1.37	1.60	1.12	
C- α	1.90	1.68	1.19	1.16	
τ_R (ps) ^c					
DTPA moiety	37	74	98	93	
sugar chain		37	56	54	

^a Values obtained at 50.3 MHz. ^b Rotational correlation times τ_R as determined by ^{13}C relaxation rates measurements of the La(III) complexes at 353 K and using eq 5.

relaxation rate of a nucleus ($1/T_{1,\text{obs}}$) is given by^{35–38}

$$\frac{1}{T_{1,\text{obs}}} = \frac{f_A}{T_{1,A}} + \frac{f_B}{T_{1,B}} \quad (3)$$

where $T_{1,A}$ and $T_{1,B}$ are the intrinsic relaxation times in the absence of exchange and f_A and f_B are the molar fractions of A and B. For exchange between more than two species, an analogous expression can be derived. Since it is only for remote nuclei that the outer-sphere contribution ($1/T_{1,\text{os}}$) becomes significant, this contribution was neglected in our study. The electron relaxation for Nd(III) is very fast ($T_{1e} \approx 10^{-13}$ s) with the result that the contact contribution to the paramagnetic relaxation is negligible. Two contributions are of importance: the “classical” dipolar relaxation and the Curie relaxation. From a simplified Solomon–Bloembergen equation³⁹ and the equation for the Curie relaxation,^{40,41} expression 4 can be derived, which

$$\frac{1}{T_1} = \left[\frac{4}{3} \left(\frac{\mu_0}{4\pi} \right)^2 \mu^2 \gamma_I^2 \beta^2 T_{1e} + \frac{6}{5} \left(\frac{\mu_0}{4\pi} \right)^2 \frac{\gamma_I^2 H_0^2 \mu^4 \beta^4}{(3kT)^2} \tau_R \right] \frac{1}{r^6} \quad (4)$$

relates the relaxation rate for each isomer to its structure. The first term between the brackets represents the “classical” dipolar contribution, and the second term, the Curie contribution. Here $\mu_0/4\pi$ is the magnetic permeability in a vacuum, μ is the effective magnetic moment of the lanthanide ion, γ_I is the magnetogyric ratio of the nucleus under study, β is the Bohr magneton, T_{1e} is the electron spin relaxation time, r is the distance between the ^{13}C nucleus in question and the lanthanide ion, H_0 is the magnetic field strength, k is the Boltzmann constant, T is the temperature, and τ_R is the rotational tumbling time of the complex. The contribution of the Curie spin mechanism to the total relaxation becomes significant for larger molecules (τ_R increases), particularly at higher fields.

The relative paramagnetic relaxation rates (Table 4) are about the same for all ligands studied, and they are also the same as those for the previously studied Nd(DTPA-BPA), which is

known to be 8-coordinate.²⁰ These data, therefore, support the conclusions from the Ln(III)-induced water ^{17}O shifts: The Ln(III) ion is coordinated by the ligand in an octadentate binding mode via three carboxylate oxygens, two amide oxygens, and the three nitrogens of the diethylenetriamine unit. Additionally, the low relaxation rates of the sugar side chains indicate that the hydroxyl groups of the ligands are not involved in the coordination of Ln(III).

If τ_R and T_{1e} are known, the absolute distances between Nd(III) and the ligand nuclei can be calculated from the relaxation rates and eq 4. The value of τ_R , under the conditions applied, can be estimated from the intramolecular dipole–dipole relaxation rate ($1/T_{1,\text{DD}}$) of a ^{13}C nucleus of the ligand in the corresponding diamagnetic La(III) complex using eq 5:

$$\frac{1}{T_{1,\text{DD}}} = N \left(\frac{\mu_0}{4\pi} \right)^2 \frac{\hbar^2 \gamma^2 [^{13}\text{C}] \gamma^2 [^1\text{H}]}{r_{\text{CH}}^6} \tau_R \quad (5)$$

Here \hbar is the Dirac constant and N is the number of protons bound to the ^{13}C nucleus. The dipole–dipole contribution to the observed relaxation rate ($1/T_{1,\text{obs}}$) was determined from the diamagnetic relaxation rate using eq 6, in which η_{obs} is the

$$\frac{1}{T_{1,\text{DD}}} = \frac{\eta_{\text{obs}}}{1.986 T_{1,\text{obs}}} \quad (6)$$

nuclear Overhauser enhancement. In Table 4 the τ_R values for the various ligands as determined from ^{13}C relaxation rates in the corresponding La(III) complexes are summarized. The increase in molecular weight is clearly reflected in the increase of τ_R going from DTPA-BEA $^{3-}$ to DTPA-BENGALAA $^{3-}$ via DTPA-BPDA $^{3-}$ and DTPA-BGLUCA $^{3-}$. The molecular weights of DTPA-BGLUCA $^{3-}$ and DTPA-BENGALAA $^{3-}$ have the same magnitude; consequently, the rotational correlation times of these chelates are similar. The results show that, in all ligands, the DTPA-backbone rotates approximately twice as slow as the sugar entity.

It has been shown that the T_{1e} value is usually rather independent of the ligation of the Ln(III) cation.^{33,42,43} For lanthanides other than Gd, large deviations from T_{1e} are only expected for complexes that are very rigid and for symmetrical

(35) Zimmerman, J. R.; Brittin, W. E. *J. Phys. Chem.* **1957**, *61*, 1328.

(36) Swift, T. J.; Connick, R. E. *J. Chem. Phys.* **1962**, *37*, 307.

(37) Leigh, J. S., Jr. *J. Magn. Reson.* **1971**, *4*, 308.

(38) McLaughlin, A. C.; Leigh, J. S., Jr. *J. Magn. Reson.* **1973**, *9*, 296.

(39) Reuben, J.; Fiat, D. *J. Chem. Phys.* **1969**, *51*, 4918.

(40) Gueron, M. *J. Magn. Reson.* **1975**, *19*, 58.

(41) Vega, A. J.; Fiat, D. *Mol. Phys.* **1976**, *31*, 374.

(42) Alsaadi, B. M.; Rossotti, F. J. C.; Williams, R. J. P. *J. Chem. Soc., Dalton Trans.* **1980**, 2147.

(43) Burns, P. D.; LaMar, G. N. *J. Magn. Reson.* **1982**, *46*, 61.

Table 5. Nd(III)–C Distances, r (Å), in the Isomers of Nd Complexes of the Ligands Concerned and Comparison with Distances in the Nd(DTPA)²⁻ and Nd(DTPA-BPA) Complexes and in the Solid-State Structure of Gd(DTPA-EA₂)

complex	CO	CH ₂ CO	NCH ₂ CH ₂ N	C-α
Nd(DTPA-BEA)	3.14–3.30	3.28–3.39	3.38–3.44	4.98–5.11
Nd(DTPA-BPDA)	3.04–3.28	3.25–3.55	3.33–3.43	5.21–5.53
Nd(DTPA-BGLUCA)	3.10–3.26	3.25–3.59	3.36–3.42	4.38–4.86
Nd(DTPA-BENGALAA) ^a	3.08–3.17	3.20–3.29	3.20–3.37	4.95–5.16
	3.05–3.27	3.26–3.39	3.04–3.39	
Nd(DTPA) ²⁻ ^b	3.15–3.20		3.21–3.48	
Nd(DTPA-BPA) ^c	3.08–3.19	3.25–3.37	3.36–3.43	5.33–5.47
Gd(DTPA-EA) ^d	3.25–3.31	3.40–3.56	3.46–3.51	5.13–5.23

^a Upper row values obtained at 400 MHz; lower row values obtained at 200 MHz; distances calculated with $T_{1e} = 1.5 \times 10^{-13} \text{ s}^{-1}$. ^b Reference 32. ^c Reference 20. ^d From solid-state X-ray analysis.⁸

macrocyclic ligands.⁴⁴ By use of data reported by Alsaadi et al. on Nd(III) complexes of DTPA⁵⁻ and related polyamino carboxylate ligands,³³ T_{1e} for the Nd complexes of DTPA-BEA³⁻, DTPA-BPDA³⁻, and DTPA-BGLUCA³⁻ at 80 °C is estimated to be $0.9 \times 10^{-13} \text{ s}$. Then distances r were calculated for DTPA-BEA³⁻, DTPA-BPDA³⁻, and DTPA-BGLUCA³⁻ from the paramagnetic relaxation rates using eq 4. The distances obtained are compiled in Table 5. The carbon atoms, except for the amide C-α, in the polyhydroxy chain are relatively far away from the Nd(III) ion compared with these C atoms present in the DTPA backbone. Consequently, the Nd(III)-induced relaxation rate enhancement is small causing the corresponding Nd(III)–C distances to be inaccurate; hence, these data were not considered.

The magnitudes of the relaxation rates for DTPA-BENGALAA³⁻ (Table 4) are approximately 1.7 times larger than those of the other chelates, which would result in relatively short (and therefore improbable) Nd(III)–C distances upon implementation of the procedure described above. The τ_R values obtained from the relaxation rate measurements of the LaDTPA-BENGALAA complex agree with the observed trend. This leaves a higher value for T_{1e} as an explanation for the relatively large relaxation rates in DTPA-BENGALAA³⁻. We therefore have also performed relaxation rate measurements on this ligand at lower magnetic field (4.7 T). With the use of eq 4, it can be estimated that under these conditions the contribution of the Curie mechanism to the total relaxation is negligible (<3%). On the basis of the distances in the solid-state structure of Gd(DTPA-bis(ethylamine))⁸ (Gd(DTPA-EA)) and the relaxation data obtained at 4.7 T, T_{1e} for Nd(DTPA-BENGALAA) was estimated to be $1.5 \times 10^{-13} \text{ s}$.

Variable-Temperature ¹⁷O NMR Measurements. The compositions of all the solutions used in the measurements are given in Table 1. From the measured ¹⁷O NMR relaxation rates and angular frequencies of the [Gd(DTPA-bis(amides))(H₂O)] solutions, $1/T_1$, $1/T_2$, and ω , and of the acidified water reference, $1/T_{1A}$, $1/T_{2A}$, and ω_A , one can calculate the reduced relaxation rates and chemical shifts, $1/T_{1r}$, $1/T_{2r}$, and $\Delta\omega_r$, which may be written as in eqs 7–9,^{35–38} where $1/T_{1m}$ and $1/T_{2m}$ are the relaxation rates in the bound water, $\Delta\omega_m$ is the chemical shift

$$\frac{1}{T_{1r}} = \frac{1}{P_m} \left[\frac{1}{T_1} - \frac{1}{T_{1A}} \right] = \frac{?1}{T_{1m} + \tau_m} + \frac{1}{T_{1os}} \quad (7)$$

$$\frac{1}{T_{2r}} = \frac{1}{P_m} \left[\frac{1}{T_2} - \frac{1}{T_{2A}} \right] = \frac{1}{\tau_m} \frac{T_{2m}^{-2} + \tau_m^{-1} T_{2m}^{-1} + \Delta\omega_m^2}{(\tau_m^{-1} + T_{2m}^{-1})^2 + \Delta\omega_m^2} + \frac{1}{T_{2os}} \quad (8)$$

$$\Delta\omega_r = \frac{1}{P_m} (\omega - \omega_A) = \frac{\Delta\omega_m}{(1 + \tau_m T_{2m}^{-1})^2 + \tau_m^2 \Delta\omega_m^2} + \Delta\omega_{os} \quad (9)$$

difference between the bound and bulk water (in the absence of a paramagnetic interaction with the bulk water), P_m is the mole fraction of bound water, and τ_m is the residence time of water molecules in the inner coordination sphere. The total outer-sphere contributions to the reduced relaxation rates and chemical shift are represented by $1/T_{1os}$, $1/T_{2os}$, and $\Delta\omega_{os}$.

It has been shown that the outer-sphere contributions in eqs 7 and 8 can be neglected.^{45,46} The full eqs 7 and 8 were used in the fitting of the experimental data. However, it is useful to consider the simplified eqs 10 and 11, where the contribution of $\Delta\omega_m$ in eq 8 has been neglected.

$$\frac{1}{T_{1r}} = \frac{1}{T_{1m} + \tau_m} \quad (10)$$

$$\frac{1}{T_{2r}} = \frac{1}{T_{2m} + \tau_m} \quad (11)$$

The maxima observed in the temperature dependence of $1/T_{2r}$ are characteristic of a changeover from the “fast-exchange” limit at high temperatures, where T_{2m} is the principal term in the denominator of eq 11, to the “slow-exchange” limit at low temperatures, where τ_m is the principal term. Since $T_{1m} > T_{2m}$, the maximum in $1/T_{1r}$ is shifted to lower temperatures as can be seen from the results shown in Figure 5.

The changeover between fast- and slow-exchange limits is also manifested in $\Delta\omega_r$, the maxima in $1/T_{2r}$ corresponding to the points of inflection in $\Delta\omega_r$. At high temperatures, the inner-sphere contribution to $\Delta\omega_r$ is given by the chemical shift of the bound water molecules, which is determined by the hyperfine interaction between the Gd(III) electron spin and the ¹⁷O nucleus via⁴⁷

$$\Delta\omega_m = \frac{g_L \mu_B S(S+1)B}{3k_B T} \frac{A}{\hbar} \quad (12)$$

where g_L is the isotropic Landé g -factor ($g_L = 2.0$ for Gd(III)), S is the electron spin ($S = 7/2$ for Gd(III)), A/\hbar is the hyperfine or scalar coupling constant, and B is the magnetic field. We assume that the outer-sphere contribution to $\Delta\omega_r$ has a temperature dependence similar to $\Delta\omega_m$ and is given by

$$\Delta\omega_{os} = C_{os} \Delta\omega_m \quad (13)$$

where C_{os} is an empirical constant.

The ¹⁷O longitudinal relaxation rates in Gd(III) solutions are dominated by the dipole–dipole and quadrupolar mechanisms⁴⁵

(44) Sherry, A. D.; Brown, R. D., III; Gerald, C. F. G. C.; Koenig, S. H.; Kuan, K.-T.; Spiller, M. *Inorg. Chem.* **1989**, *28*, 620.

(45) Micskei, K.; Helm, L.; Brücher, E.; Merbach, A. E. *Inorg. Chem.* **1993**, *32*, 3844.

(46) Micskei, K.; Powell, D. H.; Helm, L.; Brücher, E.; Merbach, A. E. *Magn. Reson. Chem.* **1993**, *31*, 1011.

(47) Bloembergen, N. *J. Chem. Phys.* **1957**, *27*, 595.

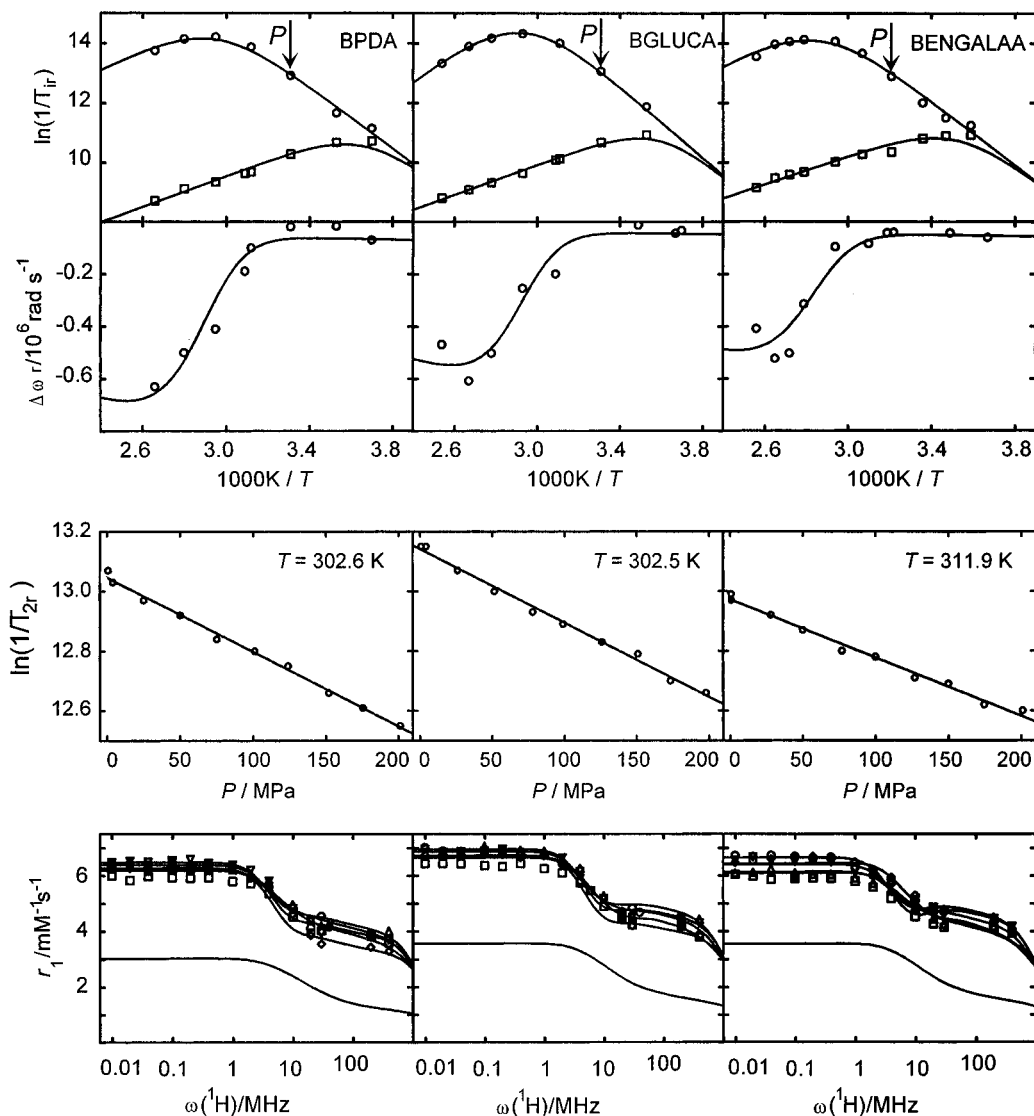


Figure 5. From top to bottom, temperature dependence of reduced ^{17}O transverse (○) and longitudinal relaxation rates (□) $\ln(1/T_{ir})$ and of chemical shifts $\Delta\omega_r$ (○), pressure dependence of transverse relaxation rates, and NMRD profiles for the complexes [Gd(DTPA-BPDA)(H₂O)], [Gd(DTPA-BGLUCA)(H₂O)], and [Gd(DTPA-BENGALAA)(H₂O)]. The curves represent simultaneous least-squares fits (see text). The temperature at which the variable-pressure experiments were performed is indicated with “P” in the top box. The lower curves in the NMRD plots represent the calculated outer-sphere contribution to the relaxivity at 298 K. NMRD profiles: 278.2 K (○); 288.2 K (□); 298.2 K (△); 308.2 K (▽); 318.2 K (◇). For individual NMRD profiles at the various temperatures, see the Supporting Information.

and, to a good approximation,⁴⁶ may be expressed by

$$\frac{1}{T_{1m}} = \left[\frac{1}{15} \left(\frac{\mu_0}{4\pi} \right)^2 \frac{\hbar^2 \gamma_I^2 \gamma_S^2}{r_{\text{GdO}}^6} S(S+1) \right] \times \left[6\tau_{d1} + 14 \frac{\tau_{d2}}{1 + \omega_S^2 \tau_{d2}} \right] + \frac{3\pi^2}{10} \frac{2I+3}{I^2(2I-1)} \chi^2 (1 + \eta^2/3) \tau_R \quad (14)$$

where $\gamma_S = g_L \mu_B / \hbar$ is the electron gyromagnetic ratio ($\gamma_S = 1.76 \times 10^{11} \text{ rad s}^{-1} \text{ T}^{-1}$ for $g_L = 2.0$), γ_I is the nuclear gyromagnetic ratio ($\gamma_I = -3.626 \times 10^7 \text{ rad s}^{-1} \text{ T}^{-1}$ for ^{17}O), r_{GdO} is the distance between the electron charge and the ^{17}O nucleus (the metal–oxygen distance in the point dipole approximation), τ_R is the rotational correlation time for the Gd(III)–O vector, $\tau_{di}^{-1} = \tau_m^{-1} + T_{ie}^{-1} + \tau_R^{-1}$, I is the nuclear spin ($I = 5/2$ for ^{17}O), χ is the quadrupolar coupling constant, and η is an asymmetry parameter. We estimate that $r = 0.25$

nm from neutron diffraction measurements of lanthanide aqua ions in solution⁴⁸ and from the X-ray crystal structure of a structural analogue [Gd(DTPA-BMA)(H₂O)]⁴⁹ of the [Gd-(DTPA-bis(amide))(H₂O)] complexes investigated.

We assume that the rotational correlation time, τ_R , has a simple exponential temperature dependence as in eq 15, where τ_R is the correlation time at 298.15 K and E_R is the activation energy.

$$\tau_R = \tau_R^{298} \exp \left[\frac{E_R}{R} \left(\frac{1}{T} - \frac{1}{298.15} \right) \right] \quad (15)$$

The ^{17}O transverse relaxation rates in Gd(III) bound water molecules are dominated by the scalar relaxation mechanism^{45,50} and obey to a very good approximation the following relation-

(48) Helm, L.; Merbach, A. E. *Eur. J. Solid State Inorg. Chem.* **1991**, *28*, 245.

(49) González, G.; Powell, D. H.; Tissières, V.; Merbach, A. E. *J. Phys. Chem.* **1994**, *98*, 53.

(50) Southwood-Jones, R. V.; Earl, W. L.; Newman, K. E.; Merbach, A. E. *J. Chem. Phys.* **1980**, *73*, 5909.

ship:⁴⁶

$$\frac{1}{T_{2m}} = \frac{S(S+1)}{3} \left(\frac{A}{\hbar} \right)^2 \left(\tau_{1s} + \frac{\tau_{2s}}{1 + \omega_s^2 \tau_{2s}^2} \right) \quad (16)$$

where $\tau_{1s}^{-1} = \tau_m^{-1} + T_{ie}^{-1}$. It should be noted that the scalar mechanism is unimportant in the longitudinal relaxation and in proton relaxations.⁵¹

The binding time (or exchange rate, k_{ex}) of water molecules in the inner sphere is assumed to obey the Eyring equation as written in eq 17, where ΔS^\ddagger and ΔH^\ddagger are the entropy and enthalpy of activation for the exchange process and k_{ex}^{298} is the exchange rate at 298.15 K.

$$\frac{1}{\tau_m} = k_{ex} = \frac{k_B T}{h} \exp \left[\frac{\Delta S^\ddagger}{R} - \frac{\Delta H^\ddagger}{RT} \right] = \frac{k_{ex}^{298} T}{298.15} \exp \left[\frac{\Delta H^\ddagger}{R} \left(\frac{1}{298.15} - \frac{1}{T} \right) \right] \quad (17)$$

Recently, it has been shown that the electronic rates ($1/T_{ie}$) can be well described by three mechanisms (eq 18): (i) a

$$\frac{1}{T_{ie}} = \left(\frac{1}{T_{ie}} \right)^{ZFS} + \left(\frac{1}{T_{ie}} \right)^{SR} + \left(\frac{1}{T_{ie}} \right)^{inter} \quad (18)$$

relaxation mechanism arising from modulation of a static or transient zero field splitting (ZFS);⁵² (ii) a spin rotation (SR) mechanism;^{53,54} (iii) an intermolecular dipole-dipole mechanism.⁵¹ It should be noted that the transverse electronic rates have a negligible influence on the ¹⁷O (and ¹H) relaxation rates. Furthermore, it has been demonstrated that the intermolecular contribution to the longitudinal electronic relaxation rates is unimportant. It has been shown that the ZFS mechanism of longitudinal electronic relaxation to a good approximation should be a single exponential that can be described by eqs 19 and 20,⁵⁵ where ω_s is the Larmor frequency, Δ^2 is the trace of

$$\left(\frac{1}{T_{ie}} \right)^{ZFS} = \frac{1}{25} \Delta^2 \tau_v [4S(S+1) - 3] \times \left(\frac{1}{1 + \omega_s^2 \tau_v^2} + \frac{4}{1 + 4\omega_s^2 \tau_v^2} \right) \quad (19)$$

$$\left(\frac{1}{T_{2e}} \right)^{ZFS} = \Delta^2 \tau_v \left(\frac{5.26}{1 + 0.372\omega_s^2 \tau_v^2} + \frac{7.18}{1 + 1.24\omega_s^2 \tau_v^2} \right) \quad (20)$$

the square of the ZFS tensor, and τ_v is the correlation time for the modulation of ZFS. The modulation of the ZFS may be due to the lifetime of transient distortions,⁵⁶ and we assume

- (51) Powell, D. H.; Ni Dhubhghaill, O. M.; Pubanz, D.; Helm, L.; Lebedev, Y. S.; Schlaepfer, W.; Merbach, A. E. *J. Am. Chem. Soc.* **1996**, *118*, 9333.
 (52) Powell, D. H.; Merbach, A. E.; González, G.; Brücher, E.; Micskei, K.; Ottaviani, M. F.; Köhler, K.; von Zelewsky, A.; Grinberg, O. Ya.; Lebedev, Ya. S. *Helv. Chim. Acta* **1993**, *76*, 2129.
 (53) Atkins, P. W.; Kivelson, D. *J. Chem. Phys.* **1966**, *44*, 169.
 (54) Nyberg, G. *Mol. Phys.* **1967**, *12*, 69.
 (55) McLachlan, A. D. *Proc. R. Soc. London* **1964**, *A280*, 271.
 (56) Friedman, H. L. In *Protons and Ions Involved in Fast Dynamics Phenomena*; Laszlo, P., Ed.; Elsevier: Amsterdam, 1978, pp 27–42.

that the correlation time has Arrhenius behavior.

$$\tau_v = \tau_v^{298} \exp \left[\frac{E_v}{R} \left(\frac{1}{T} - \frac{1}{298.15} \right) \right] \quad (21)$$

The SR contribution is given approximately by eq 22,^{54,55} where $\delta g_L^2 = \sum_i \delta g_{Li}^2$, with δg_{Li} being the deviations of the g_L values along the principal axes of the g_L tensor from the free electron value.

$$\left(\frac{1}{T_{ie}} \right)^{SR} = \frac{\delta g_L^2}{9\tau_c} \quad (22)$$

Water Proton Relaxation (NMRD). The magnetic field dependences of longitudinal proton relaxation of [Gd(DTPA-BPDA)(H₂O)], [Gd(DTPA-BGLUCA)(H₂O)], and [Gd(DTPA-BENGALAA)(H₂O)] were recorded at several temperatures. The curves obtained are included in Figure 5.

Longitudinal proton relaxation rate enhancements in NMRD studies are commonly expressed as relaxivities (r_1 , in s⁻¹ mM⁻¹). The relation between r_1 and the inner- and outer-sphere contributions is given by eq 7 with $P_m = (cq)/55.5$, where c is the Gd(III) concentration in mol L⁻¹ and q is the number of inner-sphere water molecules ($q = 1$ in the compounds studied). The longitudinal relaxation rate of the inner-sphere water molecules is dominated by the dipolar interaction and is given by the Solomon–Bloembergen equation (eq 23),^{57,58} where r_{GdH}

$$\frac{1}{T_{1m}} = \frac{2}{15} \left(\frac{\mu_0}{4\pi} \right)^2 \frac{\hbar^2 \gamma_S^2 \gamma_I^2}{r_{GdH}^6} S(S+1) \times \left(\frac{3\tau_{d1}}{1 + \omega_I^2 \tau_{d1}^2} + \frac{7\tau_{d2}}{1 + \omega_S^2 \tau_{d2}^2} \right) \quad (23)$$

is the effective distance between the gadolinium electronic spin and the water protons and $\tau_{di}^{-1} = \tau_M^{-1} + \tau_R^{-1} + T_{ie}^{-1}$ ($i = 1, 2$). The rotational correlation time (τ_R) now concerns the rotation of the Gd(III)–water proton vector.

The outer-sphere contribution to the relaxivity, arising from diffusing water molecules external to the chelate complex for a 1 mM solution, can be described by eq 24:⁵⁹

$$r_{1OS} = \left(\frac{32\pi}{405} \right) \left(\frac{\mu_0}{4\pi} \right)^2 \gamma_I^2 \gamma_S^2 \hbar^2 S(S+1) \frac{N_A}{a_{GdH} D_{GdH}} [3J_{OS}(\omega_I, T_{1e}) + 7J_{OS}(\omega_S, T_{2e})] \quad (24)$$

with

$$J_{OS}(\omega, T_{je}) = \text{Re} \left\{ \left\{ 1 + \frac{1}{4} [i\omega\tau_{GdH} + (\tau_{GdH}/T_{je})]^{1/2} \right\} \left\{ 1 + [i\omega\tau_{GdH} + (\tau_{GdH}/T_{je})]^{1/2} + \frac{4}{9} [i\omega\tau_{GdH} + (\tau_{GdH}/T_{je})] + \frac{1}{9} [i\omega\tau_{GdH} + (\tau_{GdH}/T_{je})]^{3/2} \right\} \right\} \quad (25)$$

$$j = 1, 2$$

Here N_A is Avogadro's number, a_{GdH} is the distance of the closest approach of a second sphere water molecule to Gd(III), and the correlation time τ_{GdH} corresponds with a_{GdH}^2/D_{GdH} . The diffusion coefficient D_{GdH} is assumed to obey an exponential

- (57) Solomon, I. *Phys. Rev.* **1955**, *99*, 559.
 (58) Bloembergen, N.; Morgan, L. O. *J. Chem. Phys.* **1961**, *34*, 842.
 (59) Freed, J. H. *J. Chem. Phys.* **1978**, *68*, 4030.

Table 6. Parameters Obtained from Least-Squares Fits of ^{17}O NMR and NMRD Data^a

	Gd(DTPA) ^b	Gd(DTPA-BMA) ^b	Gd(DTPA-BPDA)	Gd(DTPA-BGLUCA)	Gd(DTPA-BENGALAA)
k_{ex}^{298} (10^6 s^{-1})	3.3 ± 0.2	0.45 ± 0.01	0.36 ± 0.02	0.38 ± 0.02	0.22 ± 0.01
ΔH^\ddagger (kJ mol ⁻¹)	51.6 ± 1.4	47.6 ± 1.1	41.0 ± 1.5	47.6 ± 1.3	42.5 ± 1.5
ΔS^\ddagger (J mol ⁻¹ K ⁻¹)	53.0 ± 4.7	22.9 ± 3.6	-1.1 ± 4.9	21.7 ± 4.3	0.06 ± 5.09
A/\hbar (10^6 rad s^{-1})	-3.8 ± 0.2	-3.8 ± 0.2	-4.0 ± 0.5	-3.1 ± 0.3	-2.9 ± 0.4
C_{OS}	0.18 ± 0.04	0.11 ± 0.04	0.07 ± 0.05	0.06 ± 0.05	0.07 ± 0.07
τ_{R}^{298} (ps)	58 ± 11	66 ± 11	162 ± 11	183 ± 10	265 ± 22
E_{R} (kJ mol ⁻¹)	17.3 ± 0.8	21.9 ± 0.5	21.7 ± 0.1	20.9 ± 0.1	19.7 ± 0.1
τ_{V}^{298} (ps)	25 ± 1	25 ± 1	15 ± 3	14 ± 1	16 ± 2
E_{V} (kJ mol ⁻¹)	1.6 ± 1.8	3.9 ± 1.4	2.6 ± 2.8	1.1 ± 1.7	5.5 ± 2.3
Δ^2 (10^{20} s^{-2})	0.46 ± 0.02	0.41 ± 0.02	0.48 ± 0.12	0.63 ± 0.08	0.53 ± 0.09
$10^2 \delta_{\text{GL}}^2$	1.2 ± 0.3	0.8 ± 0.2	1.4 ± 0.5	0.4 ± 0.3	0.8 ± 0.5
D_{GDH}^{298} ($10^{-10} \text{ m}^2 \text{ s}^{-1}$)	20 ± 3	23 ± 2	34 ± 3	26 ± 2	27 ± 2
E_{DGDH} (kJ mol ⁻¹)	19.4 ± 1.8	12.9 ± 2.1	20.6 ± 2.1	20.5 ± 1.6	24.1 ± 1.9
$\chi(1 + \eta^{2/3})^{1/2}$ (MHz)	14 ± 2/7.58	18 ± 2/7.58	10.2 ± 0.8/7.58	12.6 ± 0.7/7.58	11.1 ± 0.1/7.58
r_{GdO} (Å)	2.5/2.20 ± 0.09	2.5/2.12 ± 0.04	2.5/2.37 ± 0.04	2.5/2.26 ± 0.03	2.5/2.33 ± 0.04
ΔV^\ddagger (cm ³ mol ⁻¹)	12.5 ± 0.2	7.3 ± 0.2	6.7 ± 0.2 ^c	6.8 ± 0.2 ^d	5.6 ± 0.2 ^e

^a The data on Gd(DTPA) and Gd(DTPA-BMA) have been reported previously^b and are included for comparison. Italicized parameters were fixed in the least-squares fitting procedure. ^b Reference 51. ^c $T = 302.6 \text{ K}$. ^d $T = 302.5 \text{ K}$. ^e $T = 311.9 \text{ K}$.

temperature dependence (eq 26), where D_{GDH}^{298} is the diffusion coefficient at 298.15 K and E_{DGDH} is the activation energy.

$$D_{\text{GDH}} = D_{\text{GDH}}^{298} \exp\left[\frac{E_{\text{DGDH}}}{R}\left(\frac{1}{298.15} - \frac{1}{T}\right)\right] \quad (26)$$

Simultaneous Fitting of NMRD and ^{17}O NMR Data. The equations discussed above show that the ^{17}O NMR and ^1H NMRD data are influenced by a large number of parameters, many of which are common. Therefore, simultaneous fitting of the two data sets will put constraints on the common parameters. Further constraints were introduced by fixing some of the parameters. Distances between Gd(III) and coordinated water molecules usually are not dependent on the nature of other ligands coordinated. Following previous NMRD studies, r_{GDH} was fixed at 3.1 Å^{6,60} and a_{GDH} was fixed at 3.5 Å. Two fittings were performed: one with r_{GdO} fixed at 2.5 Å (see ^{17}O section) and the quadrupolar coupling constant treated as a variable and another one with the quadrupolar coupling constant fixed at 7.58 MHz and r_{GdO} treated as a variable (see below). The other parameters obtained from the two fitting procedures were independent of the choice of the fixed parameter (either r_{GdO} or the quadrupolar coupling constant). Initial attempts to fit the data with estimates of the outer-sphere contribution of the water ^1H relaxation rates obtained from NMRD measurements on the Gd(III) complex of triethylenetetramine-*N,N,N',N'',N''',N''''*-hexaacetic acid (Gd(TTHA)³⁻) did not result in an acceptable agreement between experimental data points and calculated curves. The Gd(TTHA) complex is so far considered as a standard outer-sphere system,⁶⁰ since the hydration number, q , is zero.^{18,61} Apparently, this complex is not suitable for this purpose in the present case. Therefore, the Freed equations were included into the fitting procedure to evaluate the outer-sphere contributions. Further studies on models for outer-sphere relaxivities are in progress.

To compensate for the difference in magnitude of the data, the logarithmic ^{17}O relaxation rates were weighted with a factor of 10, ^{17}O shifts with a factor of 10^{-5} , and ^1H relaxivities with unity. The results of the fits are presented in Table 6. For comparison previously published data for Gd(DTPA) and Gd(DTPA-BMA) are included. The obtained fits are also shown as the curves in Figure 5.

The values for the scalar coupling constant, A/\hbar , obtained for the presently studied systems (Table 6), are very similar to those obtained for several other Gd(III) chelate complexes with one inner-sphere water molecule^{45,49} and agree also with the F -value observed in many previous Ln(III) water ^{17}O shift studies.^{20,32}

As already has been observed, the water-exchange rate decreases dramatically from $[\text{Gd}(\text{H}_2\text{O})_8]^{3+}$ to the chelate complexes with one inner-sphere water molecule, $[\text{Gd}(\text{DTPA})(\text{H}_2\text{O})]^{2-}$, $[\text{Gd}(\text{DOTA})(\text{H}_2\text{O})]^-$, and $[\text{Gd}(\text{DTPA-BMA})(\text{H}_2\text{O})]$. The water-exchange rate, k_{ex}^{298} , is 1 order of magnitude lower for the three Gd complexes studied compared to the values for $[\text{Gd}(\text{DTPA})(\text{H}_2\text{O})]^{2-}$ and $[\text{Gd}(\text{DOTA})(\text{H}_2\text{O})]^-$.⁴⁵ The k_{ex}^{298} values for $[\text{Gd}(\text{DTPA-BPDA})(\text{H}_2\text{O})]$ and $[\text{Gd}(\text{DTPA-BGLUCA})(\text{H}_2\text{O})]$ are similar to that obtained for $[\text{Gd}(\text{DTPA-BMA})(\text{H}_2\text{O})]$,⁴⁹ but the value found for $[\text{Gd}(\text{DTPA-BENGALAA})(\text{H}_2\text{O})]$ is almost a factor of 2 lower. A positive activation entropy for a dissociative process is mainly due to the increasing disorder obtained upon breaking the metal-water bond. There are, however, also contributions arising from the arrangement of the remaining coordination sites and the disruption of the structure of the outer-sphere water at the transition state. These contributions may be different for each chelate complex. Previous studies of the $\text{Ni}(\text{CH}_3\text{CN})_6^{2+}$ ions demonstrated that the systematic errors in activation enthalpies and entropies are correlated;⁶² therefore overinterpretation of the observed differences in ΔS^\ddagger for the above six chelates should be avoided.

The rotational correlation times, τ_{R}^{298} , are increasing in the order Gd(DTPA) < Gd(DTPA-BMA) < Gd(DTPA-BPDA) < Gd(DTPA-BGLUCA) < Gd(DTPA-BENGALAA), as should be expected from the increase in molecular sizes in that order. These rotational correlation times are consistently shorter than in previous studies based on ^{17}O NMR alone.^{45,49} There is a discrepancy between rotational correlation times determined by the shape of the NMRD profiles and those determined by ^{17}O longitudinal correlation times.⁵¹ We allowed for this by treating either the quadrupolar coupling constant or the Gd-O distances as variables. This has the effect of changing the quadrupolar and the dipolar contribution to $1/T_{1r}$ (eq 14) for a given value of τ_{R} . The values thus obtained for r_{GdO} are about 10% shorter than expected from various structural studies. Furthermore, it should be noted that at the same time the distance r_{GDH} was fixed at 3.1 Å in the fitting procedure. Therefore, the obtained

(60) Geraldes, C. F. C. G.; Urbano, A. M.; Alpoim, M. C.; Sherry, A. D.; Kuan, K.-T.; Rajagopalan, R.; Maton, F.; Muller, R. N. *Magn. Reson. Imaging* **1995**, *2*, 13.

(61) Chang, C. A.; Brittain, H. G.; Telsler, J.; Tweedle, M. F. *Inorg. Chem.* **1990**, *29*, 4468.

(62) Newman, K. E.; Meyer, F. K.; Merbach, A. E. *J. Am. Chem. Soc.* **1979**, *101*, 1470.

values for the quadrupolar coupling constant and r_{GdO} should be considered with caution. Although deviations of the values of these parameters from their expected values (7.58 MHz⁶³ and 2.5 Å,⁴⁹ respectively) may well account for the discrepancy between NMRD and ¹⁷O NMR results, it is also likely that the rotational correlation time itself is different as a result of the large difference in concentration between the samples used for ¹⁷O NMR (about 0.2 M) and NMRD (about 1 mM). Recently, it has been demonstrated, with the use of ²H longitudinal relaxation rates,⁶⁴ that there is a concentration effect on rotational correlation times of paramagnetic samples, particularly above a concentration of 50 mM.⁶⁴ For example, the rotational correlation time of a solution of La(DTPA-BMA)-d₈ increases from about 75 to 100 ps upon increase of the concentration from 1 to 250 mM at 310 K.⁶⁴

The values of the diffusion constant D_{GdH}^{298} of the presently studied complexes are somewhat higher than those of Gd(DTPA)²⁻, whereas the values of τ_v are significantly lower.⁵¹ With the use of the Freed equations, it can then be calculated that the outer-sphere contributions to the relaxivities of the Gd-(DTPA-bisamide) complexes differ substantially from that of Gd(DTPA)²⁻. This may explain that Gd(TTHA)³⁻, which is a good outer-sphere model for Gd(DTPA)²⁻, is not applicable for that purpose for DTPA-bis(amide) complexes, especially for those carrying large hydrophilic groups.

The profiles recorded with the three Gd(III) complexes at 37 °C closely resemble that of Gd(DTPA)²⁻ at low fields (<10 MHz). However at higher frequencies (>20 MHz), the relaxivities for all three complexes become larger than for Gd(DTPA)²⁻. In this high-field region, the dominant parameters involved are τ_m and τ_R . The water-exchange rates of the three Gd(III) complexes are about 10 times lower compared to those of [Gd(DTPA)(H₂O)]²⁻ at 37 °C (Table 6), which should result in lower relaxivity values for the DTPA-bis(amide) complexes. The increase in τ_R values for the Gd(III) chelates investigated as compared with [Gd(DTPA)(H₂O)]²⁻ apparently overcomes the decrease in the high-field relaxivity due to the slower exchange. The relaxivities obtained for each Gd(III) complex at various temperatures demonstrate that the relaxivity is almost temperature independent, in contrast to [Gd(DTPA)(H₂O)]²⁻.⁶ Similar behavior has already been observed for several other DTPA-bis(amides).^{7,60} This insensitivity of the relaxivities of the Gd(DTPA-bis(amide)) complexes to the temperature can be ascribed to opposite signs of the temperature dependencies of the inner- and outer-sphere contributions. The inner-sphere contributions here decrease dramatically upon decrease of the temperature, mainly due to the limitation of the r_{HS} by τ_M , whereas [Gd(DTPA)(H₂O)]²⁻ displays a typical τ_R -governed relaxivity evolution with increasing relaxivity upon decrease of the temperature. The outer-sphere contributions of both Gd-(DTPA-bis(amide)) complexes and [Gd(DTPA)(H₂O)]²⁻ increase upon decrease of the temperature.

²H Longitudinal Relaxation Rates. To have an independent check on the rotational correlation times, we performed longitudinal ²H relaxation rate measurements on the deuterated ligands, which were prepared by boiling a solution of the ligand in 0.1 M K₂CO₃ in D₂O. The DTPA-BENGALAA ligand was not stable under these conditions and, therefore, will not be considered in the discussion.

The longitudinal relaxation rate is here governed by the quadrupolar mechanism and can be given by the second term

Table 7. Rotational Correlation Times at 298 K (τ_R^{298}) and Associated Activation Energies for La(III) Complexes, Obtained with 1 mM Solutions in D₂O by ²H NMR at 30.7 MHz

	DTPA	DTPA-BMA	DTPA-BPDA	DTPA-BGLUCA
τ_R^{298} (ps)	80 ± 10 ^a	89 ± 12 ^a	118.9 ± 7.0	180.4 ± 9.1
E_R (kJ mol ⁻¹)	22.4 ^a	21 ^a	22.8 ± 2.6	21.6 ± 2.3

^a Reference 67.

in eq 14. The asymmetry parameter η is negligible, and the quadrupolar coupling constant is assumed to be 170 kHz.^{65,66} The rotational correlation times obtained in this way together with their associated activation energies are given in Table 7. The values obtained are in adequate agreement with those obtained by the simultaneous fitting of the ¹⁷O NMR and NMRD data.

Variable-Pressure ¹⁷O NMR Measurements and Water Exchange Mechanism. The pressure dependence of the reduced transverse relaxation rates, $1/T_{2r}$, at temperatures between 302 and 312 K and at 9.4 T is shown in Figure 5. At this magnetic field and the temperatures chosen, the systems are in the slow-exchange limit and $1/T_{2r}$ equals τ_m . The decrease of $1/T_{2r}$ with pressure in Figure 5 is therefore due to deceleration of the water exchange process. The pressure dependence of the water exchange rate may be written as in eq 27, where ΔV_0^\ddagger

$$\frac{1}{\tau_m} = k_{\text{ex}} = (k_{\text{ex}})_0^T \exp\left[-\frac{\Delta V_0^\ddagger}{RT}P + \frac{\Delta\beta^\ddagger}{2RT}P^2\right] \quad (27)$$

is the activation volume at zero pressure and temperature T , $(k_{\text{ex}})_0^T$ is the exchange rate at zero pressure and temperature T , and $\Delta\beta^\ddagger$ is the compressibility coefficient of activation. In the fitting procedure we included a possible pressure dependence of the bound water relaxation rate $1/T_{2m}$ as given in eq 28. Upon

$$\frac{1}{T_{2m}} = \frac{1}{T_{2m}^0} \exp\left(\frac{-\Delta V_m^\ddagger}{RT}P\right) \quad (28)$$

fixing ΔV_m^\ddagger at values from -5 to +5 cm³ mol⁻¹, the results remained, within the statistical error, the same as those given in Table 6. An influence of $1/T_{2m}$ on the data can thus be excluded.

We performed a least-squares fit of the data in Figure 5 using eqs 8, 12, 15, 19, 21, 22, and 27 with $(k_{\text{ex}})_0^T$ and ΔV_0^\ddagger as fitted parameters. In previous studies,⁶⁸ the pressure dependence of $\ln(k_{\text{ex}})$ has been found to be nearly linear, so we assume that $\Delta\beta^\ddagger = 0$. The scalar coupling constant was found previously to be independent of pressure, so we assume that it is constant and equal to the value in Table 6. The fitted function is shown in Figure 5, and the corresponding obtained kinetic parameters are included in Table 6. The water exchange rates at zero pressure and temperature T compared with those calculated from the variable-temperature ¹⁷O NMR data, using eq 17, are in good agreement (Supporting Information).

The water exchange rates and their activation volumes are independent of the substitution of the DTPA backbone. The negative ΔV_0^\ddagger value for [Gd(H₂O)₈]³⁺ indicates associatively activated water exchange (I_a mechanism), whereas the large positive ΔV_0^\ddagger values for [Gd(DTPA)(H₂O)]²⁻ and [Gd-(DOTA)(H₂O)]⁻ indicate more dissociatively activated water

(63) Halle, B.; Wennerstrom, H. *J. Chem. Phys.* **1981**, *75*, 1928.

(64) Vander Elst, L.; Maton, F.; Laurent, S.; Muller, R. N., Poster presented at the Thirteenth European Experimental N. M. R. Conference, Paris, France, May 19–24, 1996, book of abstracts, p 144.

(65) Mantsch, H. H.; Saito, H.; Smith, I. C. P. *Prog. Nucl. Magn. Reson. Spectrosc.* **1977**, *11*, 211.

(66) Derbyshire, W.; Gorvin, T. C.; Warner, D. *Mol. Phys.* **1969**, *17*, 401.

(67) Muller, R. N., et al. Unpublished data.

(68) Cossy, C.; Helm, L.; Merbach, A. E. *Inorg. Chem.* **1989**, *28*, 2699.

exchange. This can be understood if we consider that the latter two chelate complexes can accommodate only one inner-sphere water molecule. The incoming water molecule cannot participate in water exchange, which will have a dissociative activation mode and probably a limiting dissociative D mechanism. Without participation of the incoming water molecule, more energy is required to break the bond between the outgoing water molecule and the highly charged Gd(III), leading to the higher ΔH^\ddagger and lower k_{ex}^{298} values. The results for the [Gd(DTPA-bis(amide)(H₂O))] complexes investigated obey this trend, and we conclude that the water exchange on these chelate complexes takes place most probably via a limiting dissociative D mechanism.

Conclusions

Replacement of the alkyl functions in Ln(III) complexes of DTPA-bis(alkylamides) by polyhydroxylated ones has no significant influence on the structure of the complex. The coordination polyhedron remains the same, and there is no interaction between the hydroxyl groups and the Ln(III) ion. The large similarity between the two classes of complexes is also reflected in the parameters determining the relaxivity of the Gd(III) complex. The rotational correlation time is determined by the molecular volume of the complex. The exchange rate is typically 1 order of magnitude smaller than that of Gd(DTPA) (see Table 6). The exchange rate shows a trend toward lower rates upon increase of the bulkiness of the amide functions. Possibly the DTPA-bis(amide) group is wrapped around the Gd(III) ion in a less tight way upon increase of the steric interactions between the amide groups. This may then lead to a decrease of the steric strain of the bound water molecule and, consequently, to an increase of the free enthalpy gap between the ground state and the eight-coordinate transition state and thus to a reduction of the water exchange rate. At the same time, the A/\hbar values obtained show a slight decreasing trend upon increase of the size of the amide groups. Since the hyperfine coupling constant is not very sensitive to structural changes around the Ln(III) ion, this is likely caused by a small increase of the average amount of Gd(III)-coordinated water, which is compensated in the fitting procedure by an adjustment of A/\hbar . The trend observed in the qF values agrees with this. This also suggests that the DTPA-bis(amide) is bound less tightly; possibly there is an increasing but small amount of a species with a detached amide function and two Gd(III) coordinated water molecules upon increase of the bulkiness of the side chains. At 37 °C, the exchange rate and the electronic relaxation rate are the limiting factors for the inner-sphere relaxivity of the Gd–DTPA-bis(amide) complexes. Accordingly, lowering the temperature results in a dramatic decrease of the inner sphere relaxivity, which is compensated by a concomitant increase of the outer-sphere relaxivity (see, for example, Figure 6).

Since there is no interaction between the Gd(III) ion and the hydroxyl groups, the distance between the mobile hydroxyl protons and the Gd(III) ion is rather large ($>5 \text{ \AA}$). The relaxation rate enhancement that these protons experience is,

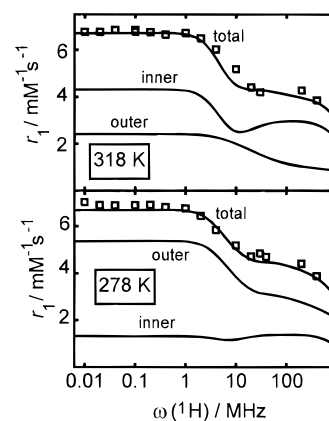


Figure 6. Comparison of the NMRD profiles of [Gd(DTPA-BGLUCA)-(H₂O)] at 318 and 278 K.

therefore, negligible, and exchange between these protons and the bulk water does not contribute to the relaxivity.

The present data allow an estimate of the relaxivities that can be expected with polysaccharides, to which Gd(DTPA) chelates are attached. The relaxivity usually increases steeply with τ_R up to 10–100 ns, where it levels off. If one uses a τ_R^{298} value of 10 ns (a typical value for a polymer), and keeps all other parameters at the values obtained for Gd(DTPA-BGLUCA), it can be calculated, with the equations described above, that $r_1 = 9.0 \text{ s}^{-1} \text{ mM}^{-1}$ (37 °C and 20 MHz). This is in good agreement with values for conjugates of dextran and Gd(DTPA).^{69–71} If it were possible to increase the water exchange rate k_{ex}^{298} from 3.8×10^5 to 2×10^7 , a further increase of r_1 to $15.2 \text{ s}^{-1} \text{ mM}^{-1}$ could be expected. A substantial increase of the relaxivity can only be achieved when the electronic relaxation parameters can be optimized, which would require alterations in the chelating unit. For example, similar calculations with the parameters for Gd(DOTA)⁵¹ give $r_1 = 29.5 \text{ s}^{-1} \text{ mM}^{-1}$ (37 °C and 20 MHz) for $\tau_R^{298} = 10 \text{ ns}$.

Acknowledgment. Thanks are due to Ms. A. M. van der Heijden and Mr. R. Demange for their contribution to synthesizing several compounds and to Drs. L. Vander Elst and S. Laurent for the ²H labeling and ²H NMR measurements. This work has been supported by the Dutch National Innovation Program Carbohydrates (IOP-K), AKZO Nobel Corporate Research, Nycomed Inc., the Swiss National Science Foundation and the Swiss OFES, the European COST D1 action (Coordination Chemistry in the Context of Biological and Environmental Studies), and the EC BIOMED 2 program (MACE).

Supporting Information Available: Tables listing ¹³C chemical shifts of Nd(DTPA-bis(amides)), variable-temperature and -pressure ¹⁷O NMR chemical shifts, longitudinal and transverse ¹⁷O relaxation data, and variable-temperature NMRD data and a Figure showing NMRD profiles at various temperatures (10 pages). Ordering information is given on any current masthead page.

IC961359K

(69) Brasch, R. C. *Magn. Reson. Med.* **1991**, *22*, 282.

(70) Rongved, P.; Klaveness, J. *Carbohydr. Res.* **1991**, *214*, 315.

(71) Chu, W.-J.; Elgavish, G. A. *NMR Biomed.* **1995**, *8*, 159.